Noninvasive monitoring with strongly absorbed light

M.P. McEwen[1, 2], K.J. Reynolds[2*]

[1]Medical Device Research Institute, School of Computer Science, Engineering and Mathematics,
 Flinders University, South Australia

[2]Biomedical Engineering Department, Flinders University School of Medicine/Flinders Medical Centre,
 South Australia

*Corresponding author: Mark.McEwen@flinders.edu.au

The transmission of light through tissue is used in noninvasive monitoring, in particular photoplethysmography. Investigations involving the transmission of wavelengths absorbed by bilirubin (short wavelength visible light) have been limited, due to strong absorption by haemoglobin. Achieving transmission of these wavelengths through tissue may advance noninvasive monitoring of substances like bilirubin. This work investigates the use of high power light sources together with improvements in signal-to-noise ratio as a means of enabling the transmission of strongly absorbed light through tissue. A custom device using multiple high-power short-wavelength visible light sources together with low power red and infrared sources, and background light cancellation – to improve signal-to-noise ratio, was constructed. Transmission of 454–1200 nm light through tissue was achieved, with pulsations present in measured signals. The transmission through tissue of multiple wavelengths of strongly absorbed light can be achieved by using high power light sources in conjunction with cancelling the effect of background light. Use of these techniques may allow investigations into the noninvasive monitoring of substances such as bilirubin using photoplethysmography.

Keywords: biomedical photonics, LED energisation, noise cancellation, photodiode, pulsed circuitry, absorption, noninvasive, photoplethysmography, pulse oximetry, transmission.

1. Introduction

The interaction of light with tissue is the basis for noninvasive monitoring instruments such as pulse oximeters [1–3]. Pulse oximetry has traditionally used red and infrared light [2, 3], which is moderately absorbed by haemoglobin [4, 5].

Observing the interaction of additional wavelengths of light with tissue may be useful because some components of blood absorb very little of the wavelengths used in pulse oximetry but absorb other wavelengths strongly, *e.g.*, bilirubin and water (Fig. 1 shows part of the bilirubin, water and haemoglobin absorption spectra). This has been investigated by several groups:
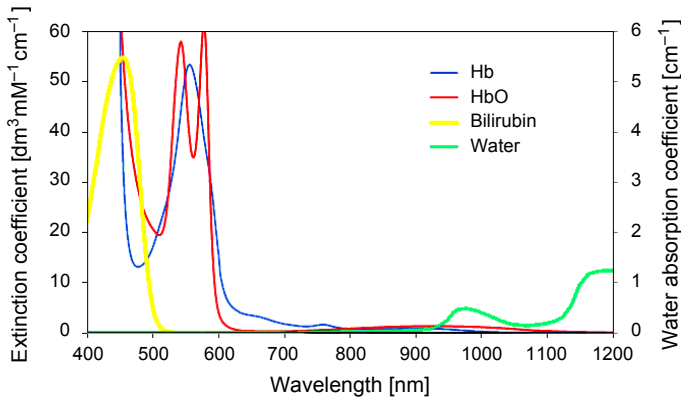
Fig. 1. Bilirubin, haemoglobin and water extinction/absorption coefficients [5, 17–23].

– Manzke *et al*. [6], Barker *et al*. [7], Macknet *et al*. [8, 9] and Suzaki *et al*. [10] used multiple red and infrared wavelengths to monitor dyshaemoglobins and total blood haemoglobin (tHb) using pulse oximetry techniques.

– Fine *et al*. [11] investigated the transmission of multiple red and infrared wavelengths (637–1310 nm) through occluded fingers for monitoring blood glucose, tHb concentration and arterial haemoglobin oxygenation (SaO_2). The reported results indicated that some features of measured signals may have been related to these blood parameters.

– Mauro *et al*. [12] investigated the use of infrared wavelengths (around 1 600 nm) for noninvasive blood glucose monitoring.

– Benaron *et al*. [13, 14] directed broadband light (blue to infrared) onto tissue, via optical fibres, and analysed the (nonpulsatile) spectrum of the reflected light, for monitoring the oxygenation of local areas of tissue.

– Jay *et al*. [15] directed white light onto tissue and analysed the (nonpulsatile) spectrum of the reflected light for noninvasively estimating tHb.

– Yoon *et al*. [16] performed photoplethysmography in transmission mode using 569 nm (yellow) and 805 nm (infrared) light for noninvasively estimating tHb.

Haemoglobin strongly absorbs light with wavelengths shorter than approximately 600 nm, and bilirubin strongly absorbs light with wavelengths shorter than approximately 500 nm (Fig. 1). This results in low transmission of these wavelengths through tissue, making investigations more difficult than when red and infrared light are used. None of the above investigations involved photoplethysmography with wavelengths of light that are absorbed by bilirubin.

Achieving the transmission of several wavelengths of light (including strongly absorbed light) through tissue may advance noninvasive monitoring, and allow the noninvasive estimation of substances such as bilirubin using photoplethysmography to be investigated more readily.

Figure 1 indicates that the oxyhaemoglobin extinction coefficient for 470 nm (blue) light is approximately 15 times larger than for 940 nm infrared light. Transmission is inversely related to the exponential of the extinction coefficient [24], hence the larger extinction coefficient for 470 nm light corresponds to a very large reduction in transmission of 470 nm, compared to 940 nm light. The use of high power light sources may increase the transmission of strongly absorbed light. For example, the Luxeon® Rebel high power 470 nm LED (LXML PB01 0013) emits 435 mW radiant power [25], whereas the 940 nm Roithner Lasertechnik LED (OPE5194WK) emits 11.3 mW radiant power [26]. That is, the high power blue LED emits approximately 40 times more power than the infrared LED. This can improve transmission of strongly absorbed light, but the improvement will only partially offset the very strong absorption, hence signals generated with these wavelengths (<600 nm) are expected to be weak. To cope with weak signals, the signal-to-noise ratio (SNR) should be maximised.

This paper describes the design of an instrument, utilising high power light sources and a noise cancellation technique, for investigating the transmission of multiple wavelengths of light (including blue, green, amber, red and infrared) through vascularised tissue. Results obtained with the device have been used to investigate the effects of blood vessel calibre and total haemoglobin (tHb) on pulse oximetry [27].

2. Methods

An instrument was made for: transmitting a broad range of light (455–1 200 nm) through tissue, measuring the intensity of light transmitted, and removing the contribution of background light to the apparent transmitted light intensity. The instrument contained a light emitting diode (LED) probe, a light sensor probe and a background light sensor. Ethics approval was obtained (Flinders Clinical Research Ethics Committee) for using the instrument on human subjects.

2.1. LED probe

Eleven LEDs were used as light sources. They were chosen from those commercially available, to include wavelengths normally used in pulse oximetry (approximately 660 and 940 nm [28]) as well as encompassing parts of the spectrum where a wide range of absorption coefficients for the major absorbers in blood (haemoglobin, bilirubin and water – Fig. 1) occurred. The LEDs used were:
1. High-power LEDs (3 mm×4.5 mm×2 mm, surface mount):
   – 455 nm, LXML-PR01-0275 (Luxeon® Rebel);
   – 470 nm, LXML-PB01-0013 (Luxeon® Rebel);
   – 505 nm, LXML-PE01-0040 (Luxeon® Rebel);
   – 530 nm, LXML-PM01-0050 (Luxeon® Rebel);
   – 590 nm, LXML-PL01-0030 (Luxeon® Rebel);
   – 620 nm, LXML-PH01-0050 (Luxeon® Rebel).

2. LEDs in a 5 mm domed casing:
   – 660 nm, L1513SRC-E (Kingbright);
   – 780 nm, ELD-780-524 (Roithner Lasertechnik);
   – 810 nm, ELD-810-525 (Roithner Lasertechnik);
   – 940 nm, OPE5194WK (Roithner Lasertechnik);
   – 1200 nm, LED1200-03 (Roithner Lasertechnik).

The high-power LEDs had large heat dissipation requirements. Normally these requirements can be met by devoting a 10 mm×10 mm circuit board area to each LED [25], but this may not be practical in the confined space of a probe. Instead the high-power LEDs were connected to extension wires in the centre of a circuit board and mounted on a heatsink (at a 10 mm pitch circle diameter (PCD)) whereas the 5 mm domed LEDs were soldered directly onto the circuit board (on a 20 mm PCD) as shown in Fig. 2. This posed a challenge regarding focusing all LEDs onto a relatively small area (*e.g.*, a fingertip).
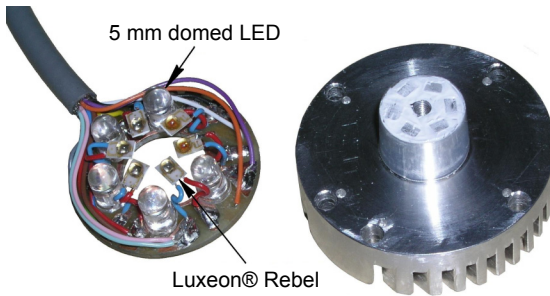

Fig. 2. LEDs connected to circuit board, and heatsink for the high-power LEDs.
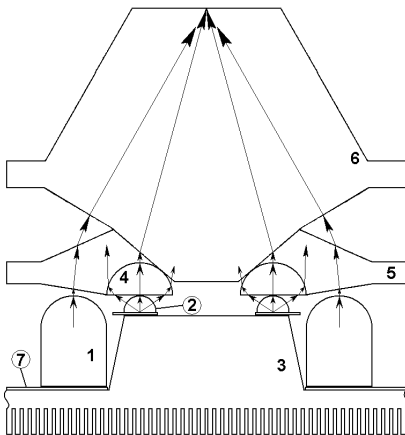

Fig. 3. Eleven LED probes cross-section, showing the light paths within the multi-part lens arrangement. 1 – 5 mm domed LED, 2 – high-power LED, 3 – aluminium heatsink, 4 – hemispherical lens, 5 – intermediate lens/holder, 6 – top lens, 7 – circuit board.

The focusing requirements for the two groups of LEDs differed. The high-power LEDs radiated light throughout wide arcs [25], and were located close to the centre of the probe. The 5 mm domed LEDs radiated light over relatively narrow arcs [26, 29–32], but were located further from the centre of the probe. A multi-part lens arrangement (Fig. 3) was used to focus and direct the output of the LEDs. Hemispherical lenses (2.5 mm radius) were used to focus light from the high-power LEDs. These lenses were held in place by an intermediate lens – which also served to partially direct the output of the 5 mm domed LEDs to the centre of the probe. A top lens directed the output of the intermediate and hemispherical lenses to the centre of the probe. Light from all LEDs was focused onto the centre of the top lens. The lens arrangement is shown in Figure 2.
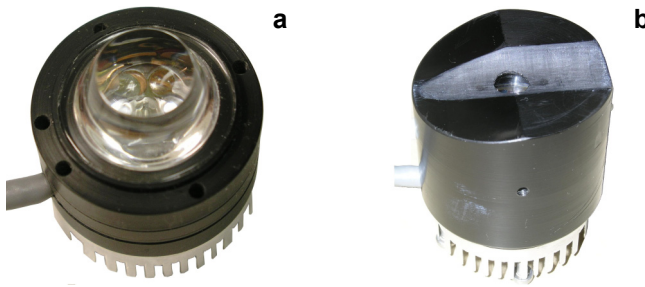

Fig. 4. LED probe, with lens uncovered (**a**) and with the retainer over the lens (**b**).

The LED probe was assembled with a retainer over the lenses (Fig. 4) which served to keep the lens components in place and to confine the light output to a small area.

2.2. Light sensor probe

To detect the wideband of wavelengths produced by the LED probe, the light sensor probe (Fig. 5) contained two photodiodes; one (Osram BPW 34 B) was sensitive to visible and short wavelength infrared light, and the other (Roithner Lasertechnik PT611) was sensitive to longer wavelength infrared light (from the 1 200 nm LED).

Spectral responses of these photodiodes are shown in Fig. 6, which identifies that photodiode sensitivity was wavelength dependent (*e.g.*, BPW 34 B response at 470 nm was approximately 50% of the response at 810 nm).
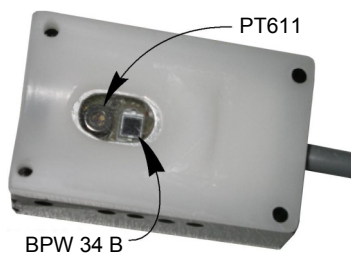

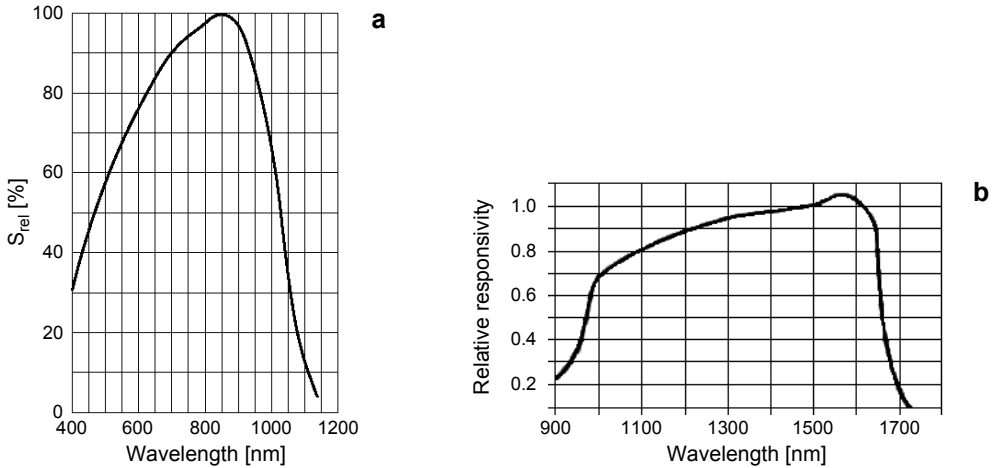Fig. 5. Light sensor probe containing PT611 and BPW 34 B photodiodes.

Fig. 6. Spectral responses of the photodiodes in the light sensor probe: BPW 34 B [33] (**a**), PT611 [34] (**b**).

Fig. 7. LED and light sensor probes in the holding fixture.

To facilitate measuring the intensity of light transmitted through tissue (*e.g.*, a finger), the LED and light sensor probes were mounted in a holding fixture, similar to a pulse oximeter finger probe (Fig. 7).

2.3. Background light sensor

The background light sensor had minor differences to the light sensor probe:
– The background light sensor was mounted remotely to the light sensor probe.
– A PT511 photodiode was used in the background light sensor instead of a PT611. The PT511 had the same spectral response as the PT611 [34, 35] (Fig. 6) but had a smaller diode area. This decreased the output of the sensor for infrared light, which compensated for the greater light intensity striking the background light sensor compared to the light sensor probe.

2.4. Noise cancellation

Intermittently energising all the LEDs, in turn, provided intervals of zero excitation, where background light could be sampled. Energisation signals for the 11 LEDs, to-
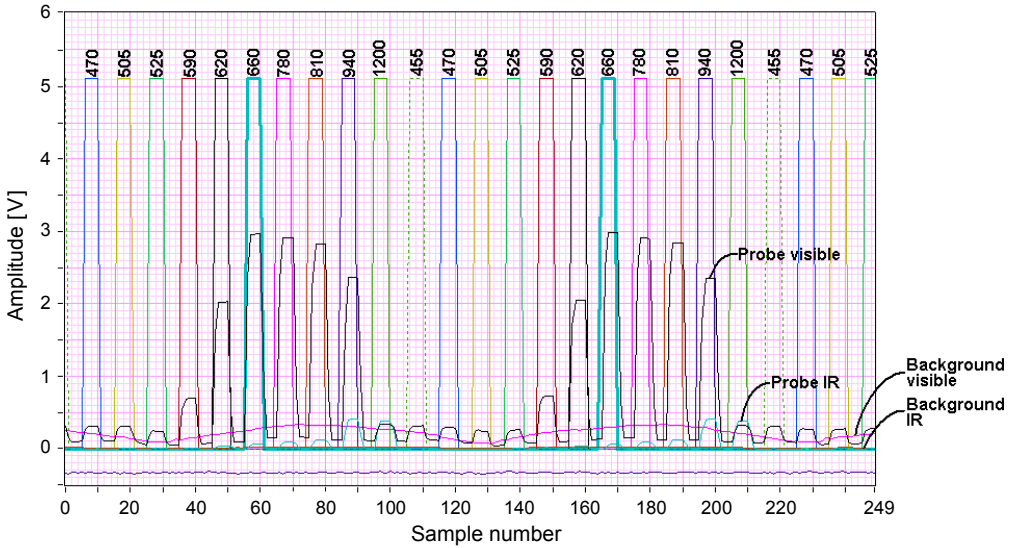
Fig. 8. LED energisation signals and visible and infrared (IR) light sensor signals.

gether with measurements from the light sensor and background light sensor, were captured. A waveform, corresponding to the intensity of transmitted light for each LED, was generated from this captured data (Fig. 8). This involved assigning the light sensor output to a LED, and removing the effect of background light by either background correction (calculated using Eqs. (1)–(3)) or baseline correction Eq. (4). Background correction was used when the minimum background light sensor output was above 0.5% of full scale, and baseline correction was used otherwise.

The waveform generation process, for the first flash of the 470 nm LED in Fig. 8 follows.

The 470 nm LED was energized at sample number 8 (Fig. 8). The outputs of the light sensor at sample number 8 were attributed to the LED plus background light. The outputs of the background light sensor immediately before and after the 470 nm LED was energized (sample numbers 4 and 14) were attributed to background lighting.

The background corrected light transmission data was calculated as:

$$\text{Background corrected data } = \text{ Light sensor output} - \overline{\beta} \times \text{Background sensor output} \tag{1}$$

The scaling factor $\overline{\beta}$ in Eq. (1) was found from the periods where LEDs were not energised. During these periods, the background light corrected data must be zero.

$$0 = \text{ Light sensor output} - \beta \times \text{Background sensor output} \tag{2a}$$

$$\therefore \beta = \frac{\text{Light sensor output}}{\text{Background sensor output}} \quad \text{(between LED pulses)} \tag{2b}$$

The scaling factor β in Eq. (2) was calculated for each interval where LEDs were not energized, and the mean value $\overline{\beta}$ before and after each period of LED energisation, was used in determining the background corrected data

$$\overline{\beta} = \frac{1}{2}\left[\frac{\text{Sensor}_{\text{pre}}}{\text{Bkgnd}_{\text{pre}}} + \frac{\text{Sensor}_{\text{post}}}{\text{Bkgnd}_{\text{post}}}\right] \tag{3}$$

where $\text{Sensor}_{\text{pre}}$ – light sensor output before LED energisation, $\text{Sensor}_{\text{post}}$ – light sensor output after LED energisation, $\text{Bkgnd}_{\text{pre}}$ – background sensor output before LED energisation, $\text{Bkgnd}_{\text{post}}$ – background sensor output after LED energisation.

The baseline corrected visible light transmission data was calculated as:

$$\text{Baseline corrected data} = \text{Sensor}_{\text{LED}} - \frac{1}{2}\left[\text{Sensor}_{\text{pre}} + \text{Sensor}_{\text{post}}\right] \tag{4}$$

where $\text{Sensor}_{\text{LED}}$ denotes light sensor output when LED energised.

2.5. Measurement procedures

Taking measurements of light transmission through an appendage (*e.g.*, a finger) with the instrument involved the following steps:

– The LED and light sensor probes and holding fixture (Fig. 7) were placed on the appendage.

– The voltages used to energize the LEDs, as well as the light and background sensor outputs were recorded every 0.1 ms, for a desired length of time.

– Background or baseline correction was applied, resulting in outputs for transmitted light intensity every 11 ms for all LEDs.

– The light sensor outputs (every 11 ms) were stored in a tab delimited data file, for subsequent analysis.

2.6. Energy delivered to tissue

The power per unit area delivered to tissue by the LED probe was calculated, for comparison to the safe exposure limit, published by the Australian Radiation Protection and Nuclear Safety Agency [36].

3. Results

Figure 9 shows an example of light transmission through a subject's finger, measured with the instrument described here. No signal processing, apart from background cancellation, was applied. No offsets were applied, but scalar multiplication of individual signals was used, to enable them to be seen clearly on the graph with minimal overlapping. The scaling factors used were: 7.1 (455 nm), 9.1 (470 nm), 12.8 (505 nm), 15.9 (525 nm), 2.4 (590 nm), 2.8 (620 nm), 2.5 (660 nm), 1.1 (780 nm), 2.1 (810 nm),
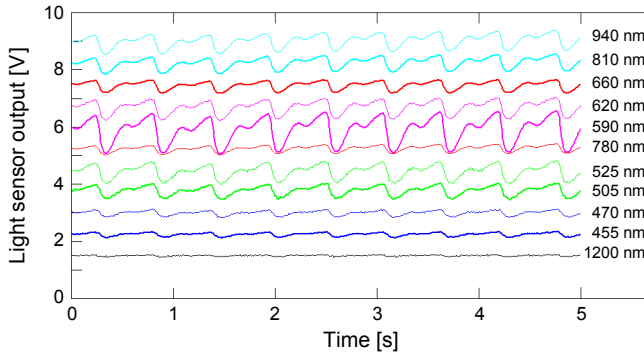
Fig. 9. Light transmission measured with the background cancellation instrument.
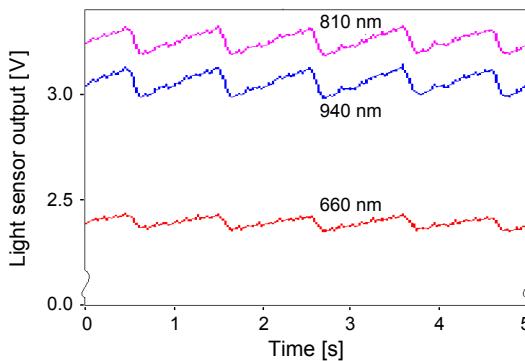

Fig. 10. Light transmission measured with a non-background cancellation instrument.

2.4 (940 nm), 9.2 (1200 nm). Figure 10 shows light transmission measurements through a subject's finger, using a similar instrument [37], that did not employ background cancellation. Less noise is evident in Fig. 9, where the data was obtained using background light cancellation.

The power per unit area delivered to tissue by the LED probe was calculated as 661 W/m^2.

4. Discussion

4.1. Design options

4.1.1. Wavelength specificity

Light from multiple, wavelength-specific sources (LEDs) was directed onto tissue one at a time, while the intensity of light emerging from tissue, was measured using a wideband light sensor. This method is employed in pulse oximeters [2, 3, 38]. The transmission of a range of wavelengths of light through tissue could also be measured by directing broad spectrum (*e.g.*, white to infrared) light onto tissue and spectrum analysing the light emerging from tissue.

Whichever of these two methods were used, very bright light would be required to achieve transmission of blue and green light through tissue. Using separate sources for each wavelength enabled bright light to be used for the wavelengths that transmit poorly through tissue, and low intensity light to be used for the more easily transmitted wavelengths. This resulted in overall lower energy delivered to tissue than could have been if a single broad spectrum bright light source were used, and was relatively inexpensive to implement.

4.1.2. Directing light onto tissue

Light from multiple sources was directed onto tissue by locating sources, together with focusing lenses and a heatsink in a probe. This could also be achieved by locating light sources, heatsinks and focusing lenses remotely and using fibre optic light guides to transport light to tissue. The fibre optic option was not used here because a miniaturized probe was not required, and low-cost was required, for the research device.

4.2. Background light

A 100 Hz component, due to fluorescent lighting used in the room, can be seen in the "background visible" signal in Fig. 8. This component is also evident in the "probe visible" signal. Testing during development of the instrument described here, demonstrated that periodic components, due to background lighting, were evident even when thick black cloth was placed over the probe.

Two methods of background light removal were used here because the level of background light can vary. In cases where the background light signal was very weak, the background cancellation algorithm, in Eqs. (1)–(3), would not be required. In fact the use of this algorithm could have been detrimental to the quality of data obtained from the system when the background light sensor output (the denominators in Eq. (3)) was very small, because very small denominators would lead to very large corrections. So any small imprecision in the estimation of the background light could lead to much larger imprecision when removing background light from signals. In these cases baseline correction, in Eq. (4), was more appropriate. Baseline correction can remove noise from signals, but if the noise changes from the time the baseline is measured (when the LED is off) to the time the signal is measured (when the LED is on), baseline correction becomes less effective and noise cancellation should be used.

The effect of background lighting may also be removed with frequency selective filters, but this can only be successful when there are no frequency components of the background light that are close to the frequency of the measured signals.

4.3. Spectral response

The wavelength dependence of photodiode response (as seen in Fig. 6) is equivalent to LED-dependent scalar multiplication of the data obtained with the photodiodes. This does not affect subsequent data analysis providing that parameters analysed are

relative to the measured signals. For instance pulsatile attenuation, as used in pulse oximetry [1], is unaffected by scalar multiplication of light sensor output – as can be seen in the following equation [1]:

$$\text{Pulsatile attenuation} \ = \ \log\left(\frac{\text{Max transmitted light intensity (diastole)}}{\text{Min transmitted light intensity (systole)}} \right) \tag{5}$$

Multiplication of the light intensity at diastole and systole by the same scalar has no effect.

4.4. Light transmission measurements

Figure 9 demonstrates that useful pulsatile transmission of blue to infrared light through tissue can be achieved when the combination of high power light sources and noise compensation is used for the wavelengths of light that are strongly absorbed by blood. The 1200 nm signal was quite weak – due to the low absorption of 1200 nm light by haemoglobin, but pulsatile components in phase with those seen in the signals from the other wavelengths are evident.

The magnitude of pulsations differed for different wavelengths, as seen in Fig. 9. This occurred because, at least in part, these magnitudes are affected by the attenuation of each wavelength by blood compared to surrounding tissue [39], and the effect of discrete blood vessels [27, 40].

The transmission of blue to infrared light through tissue, using these techniques, can enable investigations into the interaction of these wavelengths with tissue, which may advance noninvasive monitoring. By analysing pulsatile attenuations in the fingers of test subjects with known tHb and peripheral temperature, acquired with the instrument described here, a tendency for pulse oximetry to overestimate normal SaO_2 when blood vessel calibre is small and tHb is low was seen [27].

4.5. Energy delivered to tissue

Very bright LEDs were used in the instrument described here. This goes hand in hand with a risk of damaging tissue with excessive radiant energy. The Australian Radiation Protection and Nuclear Safety Agency do not publish safe exposure limits for visible and infrared light, but do publish the 8-hour exposure limit for 400 nm light onto bare skin – 1 MJ/m^2 [36]. Although the LEDs, used in the instrument described here, all emitted light with wavelengths longer than 400 nm, comparing the energy delivered to the 8-hour exposure limit for 400 nm light, provides a means of determining the safety of the instrument.

At the power per unit area delivered to tissue by the instrument described here (661 W/m^2), it would take approximately 25 minutes for the 8-hour exposure limit to be reached. This indicates that the instrument would be safe to use for measuring the light transmission through tissue for a few minutes at a time. However it should

not be placed on subjects for extended periods – as would occur if used for continuous monitoring.

5. Conclusions

The transmission through tissue, of multiple wavelengths of strongly absorbed light, can be achieved by using high power light sources in conjunction with cancellation of background light. Managing the heat dissipation requirements of multiple light sources as well as focusing their output onto tissue can be achieved by incorporating heatsinks and multi-part lenses within a probe. Use of these techniques may advance investigations into the noninvasive monitoring of substances such as bilirubin using photoplethysmography. Noninvasive monitoring devices using high powered LEDs, such as the one described here, may be safe to use for measuring the light transmission through tissue for a few minutes at a time; however the emission of large amounts of light energy, onto tissue, may exceed safe exposure levels if used for extended periods, consequently such devices should not be placed on subjects for extended periods – as would occur if used for continuous monitoring.

References

[1] Aoyagi T., *Pulse oximetry: its invention, theory, and future*, Journal of Anesthesia **17**(4), 2003, pp. 259–266.

[2] Alexander C.M., Teller L.E., Gross J.B., *Principles of pulse oximetry: theoretical and practical considerations*, Anesthesia and Analgesia **68**(3), 1989, pp. 368–376.

[3] Mendelson Y., *Pulse oximetry: theory and applications for noninvasive monitoring*, Clinical Chemistry **38**(3), 1992, pp. 1601–1607.

[4] Takatani S., Graham M.D., *Theoretical analysis of diffuse reflectance from a two-layer tissue model*, IEEE Transactions on Biomedical Engineering **26**(12), 1979, pp. 656–664.

[5] Zijlstra W., Buursma A., van Assendelft O., *Visible and Near Infrared Absorption Spectra of Human and Animal Haemoglobin*, VSP, Leiden, The Netherlands, 2000.

[6] Manzke B., Schwider J., Lutter N.O., Engelhardt K., Stork W., *Multiwavelength pulse oximetry in the measurement of hemoglobin fractions*, Proceedings of SPIE **2676**, 1996, pp. 332–340.

[7] Barker S.J., Curry J., Redford D., Morgan S., *Measurement of carboxyhemoglobin and methemoglobin by pulse oximetry: a human volunteer study*, Anesthesiology **105**(5), 2006, pp. 892–897.

[8] Macknet M., Norton S., Kimball-Jones P., Martin A.R., Allard M., *Continuous noninvasive measurement of hemoglobin via pulse CO-oximetry*, Anesthesia and Analgesia **105**, 2007, pp. S108–S109.

[9] Macknet M.R., Norton S., Kimball-Jones P.L., Applegate R.L., Martin R.D., Allard M.W., *Noninvasive measurement of continuous hemoglobin concentration via pulse CO-oximetry*, Chest **132**(4_MeetingAbstracts), 2007, pp. 493c–494c.

[10] Suzaki H., Kobayashi N., Nagaoka T., Iwasaki K., Umezu M., Takeda S., Togawa T., *Noninvasive measurement of total hemoglobin and hemoglobin derivatives using multiwavelength pulse spectrophotometry* – in vitro *study with a mock circulatory system*, 28th Annual International Conference of the IEEE Engineering in Medicine and Biology Society, EMBS '06, 2006, pp. 799–802.

[11] Fine I., Fikhte B., Shvartsman L.D., *Occlusion spectroscopy as a new paradigm for noninvasive blood measurements*, Proceedings of SPIE **4263**, 2001, pp. 122–130.

[12] MARUO K., CHIN J., TAMURA M., *Noninvasive blood glucose monitoring by novel optical-fiber probe*, Proceedings of SPIE **4624**, 2002, pp. 20–27.

[13] BENARON D.A., PARACHIKOV I.H., CHEONG W.-F., FRIEDLAND S., DUCKWORTH J.L., OTTEN D.M., RUBINSKY B.E., HORCHNER U.B., KERMIT E.L., LIU F.W., LEVINSON C.J., MURPHY A.L., PRICE J.W., TALMI Y., WEERSING J.P., *Quantitative clinical nonpulsatile and localized visible light oximeter: design of the T-Stat tissue oximeter*, Proceedings of SPIE **4955**, 2003, pp. 355–368.

[14] BENARON D.A., PARACHIKOV I.H., WAI-FUNG CHEONG, FRIEDLAND S., RUBINSKY B.E., OTTEN D.M., LIU F.W.H., LEVINSON C.J., MURPHY A.L., PRICE J.W., TALMI Y., WEERSING J.P., DUCKWORTH J.L., HÖRCHNER U.B., KERMIT E.L., *Design of a visible-light spectroscopy clinical tissue oximeter*, Journal of Biomedical Optics **10**(4), 2005, article 044005.

[15] JAY G.D., RACHT J., MCMURDY J., MATHEWS Z., HUGHES A., SUNER S., CRAWFORD G., *Point-of-care noninvasive hemoglobin determination using fiber optic reflectance spectroscopy*, 29th Annual International Conference of the IEEE Engineering in Medicine and Biology Society, EMBS '07, 2007, pp. 2932–2935.

[16] YOON G., KIM S.-J., JEON K.J., *Robust design of finger probe in non-invasive total haemoglobin monitor*, Medical and Biological Engineering and Computing **43**(1), 2005, pp. 121–125.

[17] HAI DU, RU-CHUN AMY FUH, JUNZHONG LI, CORKAN L.A., LINDSEY J.S., *PhotochemCAD: a computer -aided design and research tool in photochemistry*, Photochemistry and Photobiology **68**(2), 1998, pp. 141–142.

[18] ANDERSON R.R., PARRISH J.A., *The optics of human skin*, Journal of Investigative Dermatology **77**(1), 1981, pp. 13–19.

[19] COPE M., *The Application of Near Infrared Spectroscopy to Non Invasive Monitoring of Cerebral Oxygenation of the Newborn Infant*, Ph.D. Thesis, Department of Medical Physics and Bioengineering, University College of London, 1991, pp. 214–219.

[20] CIMPONERIU A., KAPLAN E., *Optical imaging of intrinsic signals with blue light*, SPIE's Opto Northeast and Imaging, Rochester, NY, 2001, Poster NE 03-18.

[21] BUITEVELD H., HAKVOORT J.H.M., DONZE M., *Optical properties of pure water*, Proceedings of SPIE **2258**, 1994, pp. 174–183.

[22] PALMER K.F., WILLIAMS D., *Optical properties of water in the near infrared*, Journal of the Optical Society of America **64**(8), 1974, pp. 1107–1110.

[23] LINHONG KOU, LABRIE D., CHYLEK P., *Refractive indices of water and ice in the 0.65- to 2.5-µm spectral range*, Applied Optics **32**(19), 1993, pp. 3531–3540.

[24] MEYER-ARENDT J.R., *Introduction to Classical and Modern Optics*, 2 Ed., Prentice-Hall of Australia, Sydney, 1984.

[25] *Power light source, Luxeon Rebel, Technical Datasheet DS56*, Philips Lumileds Lighting Company, 2007.

[26] *GaAlAs Infrared Emitter OPE5194WK*, Roithner Lasertechnik, 2004.

[27] MCEWEN M.P., BULL G.P., REYNOLDS K.J., *Vessel calibre and haemoglobin effects on pulse oximetry*, Physiological Measurement **30**(9), 2009, pp. 869–883.

[28] MANNHEIMER P.D., *The light-tissue interaction of pulse oximetry*, Anesthesia and Analgesia **105**(6), 2007, pp. S10–S17.

[29] *LED1200-03 Infrared LED Lamp*, Roithner Lasertechnik, 2005.

[30] *LED Lamp ELD-810-525*, Roithner Lasertechnik, 2000.

[31] *LED Lamp ELD-780-524*, EPIGAP Optoelektronik GmbH, 2008.

[32] *Solid State Lamp, L-1513SRC-E*, Kingbright, 2001.

[33] *Silicon PIN Photodiode with Enhanced Blue Sensitivity; in SMT. BPW 34 B, BPW 34 BS*, Osram, 2002.

[34] *Large Area InGaAs Photodiode Series. PT611, PT711, PT811, PT911*, Roithner Lasertechnik, 2006.

[35] *PT5xx InGaAs photodiode with 300 µm sensitive area*, Roithner Lasertechnik, 2006.

[36] *Occupational Exposure to Ultraviolet Radiation*, Radiation Protection Series Publication No. 12, Australian Radiation Protection and Nuclear Safety Agency, 2006.

[37] MacDonald R., *A Non-invasive Method for Arterial Bilirubin Measurement Using Photoplethysmography Principles*, Ph.D. Thesis, School of Computer Science Engineering and Mathematics, Flinders University, 2008.

[38] Flewelling R., *Noninvasive optical monitoring*, [In] *The Biomedical Engineering Handbook*, [Ed.] J.D. Bronzino, 2nd Ed., Vol. I, CRC Press LLC, Boca Raton, Florida, 2000, pp. 86.1–86.11.

[39] Shao Yang, Batchelder P.B., Raley D.M., *Effects of tissue outside of arterial blood vessels in pulse oximetry: a model of two-dimensional pulsation*, Journal of Clinical Monitoring and Computing **21**(6), 2007, pp. 373–379.

[40] Liu H., Chance B., Hielscher A.H., Jacques S.L., Tittel F.K., *Influence of blood vessels on the measurement of hemoglobin oxygenation as determined by time-resolved reflectance spectroscopy*, Medical Physics **22**(8), 1995, pp. 1209–1217.